A high-resolution preserving sliding-mesh approach based on meshless methods: application to acoustic propagation in presence of rotor/stator features

Sofiane Khelladi, Xesús Nogueira, Moisés Solis, Farid Bakir, Ignasi Colominas, Jacky Mardjono

ACOUSTICS 2012

A high-resolution preserving sliding-mesh approach based on meshless methods: application to acoustic propagation in presence of rotor/stator features

S. Khelladi[a], X. Nogueira[b], M. Solis[a], F. Bakir[a], I. Colominas[b] and J. Mardjono[c]

[a]DynFLuid, Arts Et Métiers-ParisTech 151 bd de l'Hopital 75013 Paris
[b]Universidade da Coruña, E.T.S.E. Camiños, Canais e Portos, campus de Elviña s/n, 15071 A Coruña, Spain
[c]Snecma, Groupe SAFRAN, SNECMA Villaroche - Bâtiment n°7D, 77550 Moissy Cramayel, France
sofiane.khelladi@ensam.eu

The acoustic hybrid approach is commonly used in the simulation of turbomachinery flows. In this technique, the aerodynamic field is solved in order to define acoustic sources, and then, these sources are propagated by solving linearised Euler equations (LEE) using a high order finite volume solver based on MLS reconstruction. One of the most widespread numerical techniques used in the numerical simulations of rotor/stator or rotor/rotor interaction flow is the so-called sliding mesh method. This technique allows relative sliding of one grid adjacent to another grid (static or in motion). However, when a high-order method is used, the interpolation used in the sliding mesh model needs to be of, at least, the same order than the numerical scheme, in order to prevent loss of accuracy. In this work we present a sliding mesh model based on the use of Moving Least Squares (MLS) approximants. It is used with a high-order (> 2) finite volume method that computes the derivatives of the Taylor reconstruction inside each control volume using MLS approximants. Thus, this new sliding mesh model fits naturally in a high-order finite volume framework for the computation of acoustic wave propagation into turbomachinery.

1 Introduction

The acoustic hybrid approach is usually used for the computation of turbomachinery noise: the aerodynamic field is solved in order to define acoustic sources, and then, these sources are propagated by solving linearised Euler equations (LEE). The aim of our work is to develop a high-order finite volume solver for the computation of the two steps of the hybrid approach: the computation of turbulent flow and the resolution of the acoustic field. Our finite volume method is based on MLS reconstruction. The theoretical fundamentals of the used finite volume method were presented in [1, 2, 6, 7] and references therein. A first application of FV-MLS for turbomachinery aeroacoustics was presented in [2, 5]. Acoustic sources were obtained using a URANS approach and propagated using LEE. Only stator blades and rotating sources into the propagating medium were considered. This first tentative permits use to study the attenuation due to the acoustic screen effect of stator blades. The next step is to introduce the rotating part into the propagation medium by the use of sliding mesh method coupled to FV-MLS solver.

One numerical technique used in the numerical simulations of rotor/stator or rotor/rotor interaction flow is the so-called sliding mesh [10, 4] method. This technique allows relative sliding of one grid adjacent to another grid (static or in motion). Thus, non-matching cells [8, 9]may appear at the interface between static and moving grids. This introduces a problem of interpolation. In addition, when a high-order method is used, the interpolation used in the sliding mesh model needs to be of, at least, the same order than the numerical scheme, in order to prevent loss of accuracy. In this work we present a sliding mesh model based on the use of Moving Least Squares (MLS) approximants [3]. It is used with a high-order (> 2) finite volume method that computes the derivatives of the Taylor reconstruction inside each control volume using MLS approximants [1, 2, 6, 7]. Thus, this new sliding mesh model fits naturally in a high-order finite volume framework for the computation of acoustic wave propagation into turbomachinery.

The paper is organized as follows. In section 2, the Moving Least Squares (MLS) approximation and the FV-MLS method are briefly described. The new MLS-based sliding-mesh technique is presented in section 3. Then, section 4 is devoted to numerical simulations. Finally, the conclusions are drawn in section 5.

2 Moving Least Squares (MLS) approximation

For clarity, in the following exposition, we consider a single variable u, instead of the vector-variable $\mathbf{U}$ used in Navier-Stokes or LEE equations. If we consider a function $u(\mathbf{x})$ defined in a domain Ω, the basic idea of the MLS approach is to approximate $u(\mathbf{x})$, at a given point $\mathbf{x}$, through a weighted least-squares fitting of $u(\mathbf{x})$ in a neighborhood of $\mathbf{x}$ as

$$u(\mathbf{x}) \approx u^h(\mathbf{x}) = \sum_{i=1}^{m} p_i(\mathbf{x})\,\alpha_i(\mathbf{z})\Big|_{\mathbf{z}=\mathbf{x}} = \mathbf{p}^T(\mathbf{x})\,\alpha(\mathbf{z})\Big|_{\mathbf{z}=\mathbf{x}} \quad (1)$$

$\mathbf{p}^T(\mathbf{x})$ is a (usually) polynomial basis and $\alpha(\mathbf{z})\Big|_{\mathbf{z}=\mathbf{x}}$ is a set of parameters to be determined, such that they minimize the following error functional:

$$J\left(\alpha(\mathbf{z})\Big|_{\mathbf{z}=\mathbf{x}}\right) = \int_{\mathbf{y}\in\Omega_{\mathbf{x}}} W(\mathbf{z}-\mathbf{y},h)\Big|_{\mathbf{z}=\mathbf{x}} \left[u(\mathbf{y}) - \mathbf{p}^T(\mathbf{y})\alpha(\mathbf{z})\Big|_{\mathbf{z}=\mathbf{x}}\right]^2 d\Omega_{\mathbf{x}} \quad (2)$$

where $W(\mathbf{z}-\mathbf{y},h)\Big|_{\mathbf{z}=\mathbf{x}}$ is a *kernel* with compact support (denoted by $\Omega_{\mathbf{x}}$) centered at $\mathbf{z}=\mathbf{x}$. The parameter h is the smoothing length, which is a measure of the size of the support $\Omega_{\mathbf{x}}$ [1]. The role of the kernel is to weight the importance of the different points used for the approximation. The minimization of J gives the following:

$$\int_{\mathbf{y}\in\Omega_{\mathbf{x}}} \mathbf{p}(\mathbf{y})W(\mathbf{z}-\mathbf{y},h)\Big|_{\mathbf{z}=\mathbf{x}} u(\mathbf{y})d\Omega_{\mathbf{x}} = \mathbf{M}(\mathbf{x})\alpha(\mathbf{z})\Big|_{\mathbf{z}=\mathbf{x}} \quad (3)$$

where the moment matrix $\mathbf{M}(\mathbf{x})$ is defined as

$$\mathbf{M}(\mathbf{x}) = \int_{\mathbf{y}\in\Omega_{\mathbf{x}}} \mathbf{p}(\mathbf{y})\mathbf{W}(\mathbf{z}-\mathbf{y},\mathbf{h})\Big|_{\mathbf{z}=\mathbf{x}} \mathbf{p}^{\mathbf{T}}(\mathbf{y})\mathbf{d}\Omega_{\mathbf{x}} \quad (4)$$

Integrals in equations (3) and (4) are evaluated using the nodes in $\Omega_{\mathbf{x}}$ ($n_{\mathbf{x}}$) as quadrature points, to obtain the following value of α

$$\alpha(\mathbf{z})\Big|_{\mathbf{z}=\mathbf{x}} = \mathbf{M}^{-1}(\mathbf{x})\mathbf{P}_{\Omega_{\mathbf{x}}}\mathbf{W}(\mathbf{x})\mathbf{u}_{\Omega_{\mathbf{x}}} \quad (5)$$

where the matrix

$$\mathbf{u}_{\Omega_{\mathbf{x}}} = \left(u(\mathbf{x_1})\cdots u(\mathbf{x}_{\mathbf{n}_{\mathbf{x}_I}})\right) \quad (6)$$

contains the nodal values of $u(\mathbf{x})$ associated to the $n_{\mathbf{x}}$ nodes in $\Omega_{\mathbf{x}}$ (figure 1). In the above, $n_{\mathbf{x}_I}$ is the number of neighbors of the cell I.

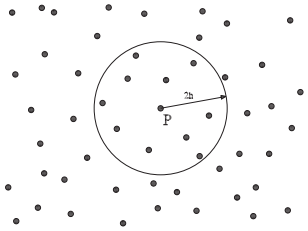

Figure 1: Meshfree approximation: general scheme. Support for reconstruction at P.

Thus, the discrete expression of the moment matrix is $\mathbf{M} = \mathbf{P}_{\Omega_\mathbf{x}}\mathbf{W}(\mathbf{x})\mathbf{P}^\mathbf{T}_{\Omega_\mathbf{x}}$ (see [1]).

We also define the matrices (see [1]):

$$\mathbf{P}_{\Omega_\mathbf{x}} = \left(\mathbf{p}(\mathbf{x_1}) \cdots \mathbf{p}(\mathbf{x}_{\mathbf{n}_{\mathbf{x_I}}})\right) \tag{7}$$

and

$$\mathbf{W}(\mathbf{x}) = \mathbf{diag}(\mathbf{W_i}(\mathbf{x})) \qquad \mathbf{i} = \mathbf{1}, \cdots, \mathbf{n}_{\mathbf{x_I}}. \tag{8}$$

From a practical point of view, for each point I we need to define a set of neighbors inside the compact support $\Omega_\mathbf{x}$. The minimum number of neighbors is determined by the number of functions in the polynomial basis $\mathbf{p}(\mathbf{x})$. The stencil used is schematically plotted in figure 2:

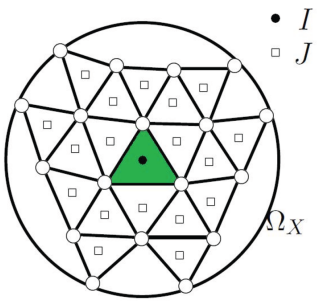

Figure 2: Stencil for reconstruction at I.

Following [1], the interpolation structure can be identified as

$$u_I{}^h(\mathbf{x}) = \mathbf{p}^T(\mathbf{x})\,\alpha(\mathbf{z})\Big|_{\mathbf{z}=\mathbf{x}} = \mathbf{p}^\mathbf{T}(\mathbf{x})\mathbf{M}^{-1}(\mathbf{x})\mathbf{P}_{\Omega_\mathbf{x}}\mathbf{W}(\mathbf{x})\mathbf{u}_{\mathbf{\Omega_x}} = \mathbf{N}^\mathbf{T}(\mathbf{x})\mathbf{u}_{\mathbf{\Omega_x}} \tag{9}$$

The MLS "shape functions" are defined as:

$$\mathbf{N}^\mathbf{T}(\mathbf{x}) = \mathbf{p}^\mathbf{T}(\mathbf{x})\mathbf{M}^{-1}(\mathbf{x})\mathbf{P}_{\Omega_\mathbf{x}}\mathbf{W}(\mathbf{x}) \tag{10}$$

and finally we can write:

$$u_I{}^h(\mathbf{x}) = \sum_{j=1}^{n_{\mathbf{x}_I}} N_j(\mathbf{x})u_j \tag{11}$$

The approximation is written in terms of the MLS "shape functions" $\mathbf{N}^\mathbf{T}(\mathbf{x})$. In this work the following polynomial cubic basis is used:

$$\mathbf{p}(\mathbf{x}) = \left(\mathbf{1}, \mathbf{x}, \mathbf{y}, \mathbf{xy}, \mathbf{x^2}, \mathbf{y^2}, \mathbf{x^2y}, \mathbf{y^2x}, \mathbf{x^3}, \mathbf{y^3}\right) \tag{12}$$

where (x, y) are the Cartesian coordinates of vector $\mathbf{x}$. Note that extension for 3D is straightforward.

In order to improve the conditioning, the polynomial basis is locally defined and scaled: if the shape functions are evaluated at $\mathbf{x}_I$, the polynomial basis is evaluated at $(\mathbf{x} - \mathbf{x}_I)/h$. With this coordinate transformation, the MLS shape functions can be written as:

$$\mathbf{N}^\mathbf{T}(\mathbf{x}) = \mathbf{p}^\mathbf{T}(\mathbf{0})\mathbf{C}(\mathbf{x_I}) = \mathbf{p}^\mathbf{T}(\mathbf{0})\mathbf{M}^{-1}(\mathbf{x_I})\mathbf{P}_{\Omega_{\mathbf{x_I}}}\mathbf{W}(\mathbf{x_I}) \tag{13}$$

with

$$\mathbf{C}(\mathbf{x}) = \mathbf{M}^{-1}(\mathbf{x})\mathbf{P}_{\Omega_\mathbf{x}}\mathbf{W}(\mathbf{x}) \tag{14}$$

2.0.1 MLS-based Finite volume method

MLS method has been used also to develop high-order finite volume methods (FV-MLS). In a finite volume framework, we need to compute the derivatives in order to perform the reconstruction of the variables at interfaces using Taylor series. In this case, the derivatives of $\mathbf{N}^\mathbf{T}(\mathbf{x})$ can be used to compute an approximation to the derivatives of the function. So, the gradient of $u^h(\mathbf{x})$ at cell I is evaluated as

$$\nabla u_I{}^h(\mathbf{x}) = \sum_{j=1}^{n_{\mathbf{x}_I}} u_j \nabla N_j(\mathbf{x}) \tag{15}$$

With Moving Least-Squares we can build a the spatial representation of the solution. This approximation gives us a continuous, highly-accurate and centered representation of the solution. Thus, a direct evaluation of the fluxes is possible, and in fact, it is efficient when the problem is not predominantly hyperbolic. Note that in case of the Navier-Stokes equations, we can compute directly viscous terms at integration points using MLS. For convection-dominated problems, we use a different approximation for hyperbolic and elliptic terms. Thus, for hyperbolic terms we *"break"* the reconstruction (via Taylor series). Thus, we approximate the variable locally inside each cell I, and this approximation is discontinuous across cell interfaces [1]. This approximation allows us to use the powerful and efficient Riemann solvers technology, limiters and other finite volume techniques. More details about the FV-MLS method can be found in [1, 2, 5, 6, 7].

3 Sliding mesh

Sliding mesh technique requires two meshed zones. In a turbomachine, one of them is related to the stator (fixed) and the other is related to the rotor (moving). The rotating grid *slides* over the fixed grid. The sliding takes place on a plane that is called *interface*. Note that in practice, the interface is composed by two coincident edges (faces in 3D). One of them belongs to the fixed grid and the other to the moving mesh.

When this technique is applied, the mesh is no longer conformal. An Arbitrary Lagrangian-Eulerian (ALE) method is used to write the conservation equations in the two meshed regions. Note that the mesh movement is not continuous, since each time step the moving region is displaced a small distance. Then the set of conservation equations is iteratively solved until convergence. Then the moving grid is displaced again.

3.1 MLS-based sliding mesh

In this work we propose the use of MLS to compute the interpolations required at the interface. The first step is to identify the neighboring cells in order to know the

stencil for the computation of MLS-shape functions. We call intersection nodes to nodes placed at interface between the moving mesh and the fixed mesh.

3.1.1 Recursive searching of intersection nodes

We call main interface to the interface edge (face in 3D) that is part of the moving mesh, and secondary interface to the interface edge that belongs to the fixed mesh (see figure 3).

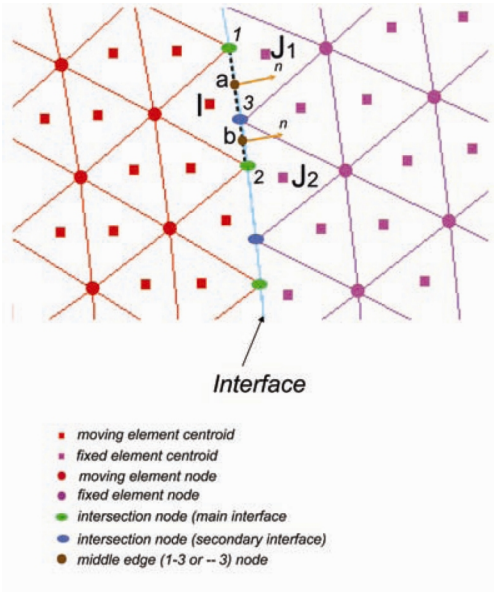

Figure 3: Schematic representation of MLS-based sliding mesh

First, we identify the "main interface"edges, with a loop over the edges of the moving mesh. If one edge is labeled as interface edge, the secondary interface is straightforwardly determined. Once the main and secondary interfaces are determined, we find intersection nodes.

3.1.2 Computation of the numerical flux at interface

The exchange of information between the moving domain and the fixed one is made at the interface (main and secondary). In a finite volume framework it is required the computation of a numerical flux at the interface between two elements. In the sliding mesh framework, as the mesh is not conformal at the interface between moving and fixed domains, the numerical flux is split in several parts there.

For example, for the cell I in figure 3, node 3 is identified as an intersection node. We compute the length of the edge formed by nodes 1 and 3, its normal and the middle node of this edge (a) (see figure 3). MLS reconstruction is applied to obtain the MLS-shape functions and their derivatives for the reconstruction of the variables at the interface of cell I. For this node, the stencil is comprised by the union of the stencils of the cell I, and all the fixed elements formed with node 3. The same rationale is applied to the segment formed with nodes 2 and 3. Numerical fluxes at interface are computed using the reconstructed using Taylor reconstructions at middle nodes a and b .

This procedure must be performed each time step. In problems related with rotor/stator configurations, the location of interface is known a priori, and also the cells next to it in both domains, fixed and moving. Thus, the computational cost is not greatly increased, since the number of cells to explore in order to identify the intersection nodes is reduced.

4 Numerical Examples

In this section we present a first test case of the new MLS-based sliding mesh technique for the Navier-Stokes equations. It is a 2D version of the real geometry of a centrifugal pump. In figure 4 we show the grid used in this example, and we identify the moving and the static domains, and also the interfaces and inlet and outlet boundaries. The moving grid has 16988 elements and fixed grid has 9972 elements.

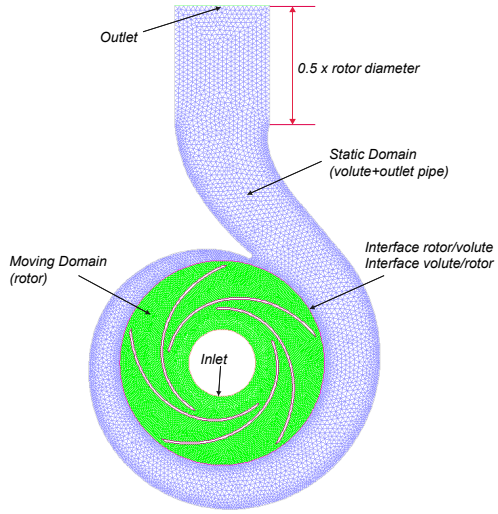

Figure 4: Schematic representation of MLS-based sliding mesh

Mass flow at inlet is $\dot{m} = 99.82\ Kg/s$. We set a value of the pressure at outlet boundary of $1.013 \times 10^5\ Pa$. In moving and fixed walls we impose the no-slip condition. The angular velocity of the rotor is 900 rpm.

In figure 5 we show the contours of the static pressure for two different time instants. We observe that the maximum value of the static pressure is found close to the "beak" of the volute, and that the pressure is uniform at outlet region.

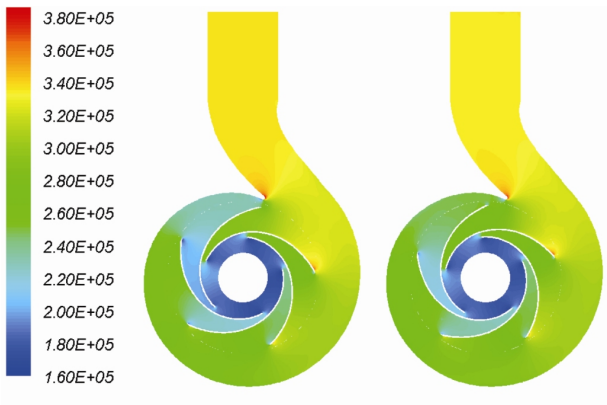

Figure 5: Contours of static pressure (Pa) in the centrifugal pump

Figure 6 shows the relative velocity field. Vortical

structures are formed in the inter-blade area, and they propagate to the outlet pipe. We observe that the solution is free of perturbations.

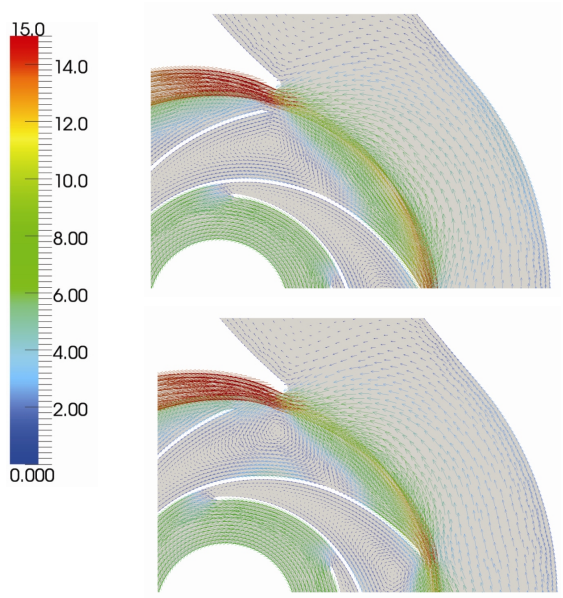

Figure 6: Relative velocity field (m/s)

5 Conclusion

In this work we have presented a new sliding-mesh technique based on Moving-Least Squares approximations. This technique allows computations on grids with non-matching cell-faces. One advantage of this approach is that it allows to maintain the accuracy of the reconstruction, avoiding low-order reconstructions at the interface between moving and fixed domains. Moreover, the same interpolation method is used in the whole domain. Thus, this new sliding mesh approach fits naturally in a high-order MLS-based finite volume framework for the computation of turbulent flow and acoustic wave propagation into turbomachinery.

Acknowledgments

This work has been partially supported by the *Ministerio de Ciencia e Innovación* (grant #DPI2009-14546-C02-01 and #DPI2010-16496), by R&D projects of the *Xunta de Galicia* (grants #CN2011/002, #PGDIT09MDS00718PR and #PGDIT09REM005118PR) cofinanced with FEDER funds, and the *Universidade da Coruña*.

References

[1] L. Cueto-Felgueroso, I. Colominas, X. Nogueira, F. Navarrina, M. Casteleiro, "Finite volume solvers and Moving Least-Squares approximations for the compressible Navier-Stokes equations on unstructured grids", *Computer Methods in Applied Mechanics and Engineering*, **196**:4712-4736 (2007).

[2] S. Khelladi, X. Nogueira, F. Bakir, I. Colominas, "Toward a Higher Order Unsteady Finite Volume Solver Based on Reproducing Kernel Methods", *Computer Methods in Applied Mechanics and Engineering*, **200**:2348-2362 (2011).

[3] P. Lancaster, K. Salkauskas, "Surfaces generated by moving least squares methods", *Mathematics of Computation*, **37**(155):141-158 (1981).

[4] J.Y. Luo, A.D. Gosman, R.I. Issa, J.C. Middleton, M.K. Fitzgerald, "Full flow field computation of mixing in baffled stirred vessels", *Chemical Engineering Research and Design A*, **71**(3):342-344 (1993).

[5] X. Nogueira, S. Khelladi, I. Colominas, L. Cueto-Felgueroso, J. París, H. Gómez, "High-resolution finite volume methods on unstructured grids for turbulence and aeroacoustics" *Archives of Computational Methods in Engineering*, **18**, 315-340 (2011).

[6] X. Nogueira, L. Cueto-Felgueroso, I. Colominas, H. Gómez, F. Navarrina, , M. Casteleiro, "On the accuracy of Finite Volume and Discontinuous Galerkin discretizations for compressible flow on unstructured grids", *International Journal for Numerical Methods in Engineering*, **78**, 1553-1584 (2009).

[7] X. Nogueira, L. Cueto-Felgueroso, I. Colominas, F. Navarrina, M. Casteleiro, "A new shock-capturing technique based on Moving Least Squares for higher-order numerical schemes on unstructured grids", *Computer Methods in Applied Mechanics and Engineering*, **199**, 2544-2558 (2010).

[8] M. Rai, "A conservative treatment of zonal boundaries for Euler equation calculations", *Journal of Computational Physics*, **62**, 472-503 (1986).

[9] M. Rai, "A relaxation Approach to patched-grid calculations with the Euler equations", *Journal of Computational Physics*, **66**, 99-131 (1986).

[10] M. Rai, "Navier-Stokes simulations of rotor-stator interaction using patched and overlaid grids", *Journal of Propulsion and Power*, **3**, 387 (1987).